DOI: 10.1002/cbic.201100269

Structural Framework for the Modulation of the Activity of the Hybrid Antibiotic Peptide Cecropin A-Melittin [CA(1–7)M(2–9)] by N^{ε}-Lysine Trimethylation

M. Dolores Díaz,[a] Beatriz G. de la Torre,[b] María Fernández-Reyes,[a] Luis Rivas,[a] David Andreu,[b] and Jesús Jiménez-Barbero*[a]

The 3D structures of six linear pentadecapeptides derived from the cecropin A–melittin antimicrobial peptide CA(1–7)M(2–9) [KWKLFKKIGAVLKVL-NH_2] have been studied. These analogues are modified by ε-NH_2 trimethylation of one or more lysine residues and showed variation in both antimicrobial and cytotoxic activities, depending on the number and position of modified lysines. Since it is expected that these peptides will display a strong conformational ordering when in contact with membranes, we have investigated their structure on the basis of the data extracted from NMR experiments performed in membrane-mimetic environments. We show that inclusion of N^{ε}-trimethylated lysine residues induces a certain degree of structural flexibility, while preserving to a variable extent a largely α-helical structure. In addition, peptide orientation with respect to SDS micelles has been explored by detection of the intensity changes of peptide NMR signals upon addition of a paramagnetic probe (Mn^{2+} ions).

Introduction

The ever-increasing bacterial resistance against traditional antibiotics has stimulated the design of novel antimicrobials that act on unconventional targets, which may thus prevent cross-resistance induction. In this regard, antimicrobial peptides (AMPs) of eukaryotic origin and their synthetic analogues represent a promising alternative. As the mechanism of AMP action usually involves the disruption of a pathogen's membranes by stoichiometric interaction with phospholipids, induction of resistance is extremely unlikely, as it would require substantial changes in phospholipid composition, affecting simultaneously both enzymatic and transport systems located in the membrane.

Due to their relatively small size and often lack of post-translational modifications, the range of therapeutically useful AMP structural modifications is limited; this in turn makes the precise definition of structure–activity relationships a must in the design of optimized AMP leads.[1]

Among the different approaches to improve AMP analogues, sequence hybridization, that is, splicing together sequence stretches from AMPs with different properties, has been rather successful. This strategy was first described with cecropin A–melittin hybrids, in which the cationic N terminus of cecropin A (CA) is followed by the hydrophobic N terminus of melittin (M). The resulting hybrid AMPs exhibit substantial improvement in their antibacterial, antiparasitic and antifungal activities compared with their parent structures. However, many of them retain a residual but persistent hemolytic activity associated to the melittin fragment.[2] For most families of linear peptides (e.g., cecropins, magainins, melittin), hemolytic activity has been linked to high values of amphipathicity, hydrophobicity or helicity.[3,4]

Hybrids with CA and M moieties of various lengths (e.g., CA(1–13)M(1–3),[5] CA(1–8)M(1–12)[6] and CA(1–7)M(2–9)[7]) have been described. In earlier structure–activity studies, it was demonstrated that shortening of the 16 residues N-terminal amphipathic section of CA caused the loss of the highly structured α-helix present in the parent cecropin A. In contrast, the hydrophobic M section at the C terminus was more prone to retain the helical structure of the original peptide.[5–7]

As CA–M hybrids share the generally poor pharmacokinetic and pharmacodynamic properties of most peptides, modifications such as succinylation,[8] N-terminal fatty acid acylation[9] and inclusion of non-natural amino acids have been explored in analogues such as CA(1–7)M(2–9) in order to enhance druggability.[10]

In this regard, it is worth mentioning that N^{ε}-trimethylation of lysine, a common epigenetic modification of Lys residues, has been only rarely used in the fine-tuning of AMP activity.[11] From a molecular point of view, trimethylation involves replacing the hydrogens of an ammonium group by three considerably more hydrophobic methyl groups, thereby increasing steric bulk and decreasing the charge density around the nitrogen atom. With the exception of the report that full permethylation

[a] Dr. M. D. Díaz, Dr. M. Fernández-Reyes, Dr. L. Rivas, Prof. J. Jiménez-Barbero
Departamento de Biología Físico-Química
Centro de Investigaciones Biológicas, CSIC
Ramiro de Maeztu 9, 28040 Madrid (Spain)
E-mail: jjbarbero@cib.csic.es

[b] Dr. B. G. de la Torre, Prof. D. Andreu
Proteomics Unit, Pompeu Fabra University
Dr. Aiguader 80, 08003 Barcelona (Spain)

Supporting information for this article is available on the WWW under http://dx.doi.org/10.1002/cbic.201100269.

of melittin (both N^{α} and N^{ε} groups) fully abrogates its hemolytic activity,[12] systematic studies of this modification are scarce, particularly with a view to extracting structure–activity relationships.

In order to provide a structural framework to explain the changes in activity brought about by lysine N^{ε}-trimethylation in CA-M peptides, we have performed an NMR study of a selected group of CA(1–7)M(2–9)NH_2 analogues (Table 1) containing at least one trimethyllysine residue. Using aqueous 2,2,2-trifluoroethanol (TFE) as a membrane-like environment, we have carried out a systematic study of the 3D structures of these N^{ε}-trimethylated peptides, showing that the presence of N^{ε}-Lys(Me_3) partially decreases the stability of the α-helix, to an extent depending on the number and position of trimethylated residues. Our data suggest that N^{ε}-trimethylation is a useful modification for fine-tuning the stability and activity of CA-M hybrids and, in general, for the development of improved antibiotic peptides.

Table 1. Peptide sequences and nomenclature used in this work.

Peptide designation		Sequence	IC_{50}[a] [μM]	HC_{50}[b] [μM]
1	CA(1–7)M(2–9)	KWKL FKKIG AVLKV L-NH_2	1.8	40.2
2	K1(Me_3)	**K**WKL FKKIG AVLKV L-NH_2	3.9	77.2
3	K7(Me_3)	KWKL FK**K**IG AVLKV L-NH_2	3.7	164.0
4	K13(Me_3)	KWKL FKKIG AVL**K**V L-NH_2	3.5	157.4
5	K1,3(Me_3)$_2$	**K**W**K**L FKKIG AVLKV L-NH_2	12.8	105.0
6	K1,13(Me_3)$_2$	**K**WKL FKKIG AVL**K**V L-NH_2	8.8	82.6
7	K1,3,6,7,13(Me_3)$_5$	**K**W**K**L F**KK**IG AVL**K**V L-NH_2	>50	>200

[a] CA(1–7)M(2–9) stands for the hybrid peptide cecropin A (1–7) and melittin (2–9). Trimethylated lysine residues are in bold. All peptides in C-terminal carboxamide form. [b] Values measured in *L. donovani* in promastigotes.[13] [c] Values measured in erythrocytes.[13]

Results and Discussion

NMR spectroscopy

We have recently demonstrated that in the CA(1–7)M(2–9) hybrid judicious substitution of lysine by N^{ε}-Lys(Me_3) increase the selectivity index of the parental peptide, mostly by reduction of the hemolytic activity rather than by improvement of the antimicrobial activity (Table 1).[13]

For some membrane active toxins, it has been established that hemolytic activity is associated with the presence of a cationic site, flanked by a hydrophobic surface.[14] This rule, based exclusively on the primary sequence of the peptides, could not account for the differences observed for CA(1–7)M(2–9) (**1**) and of its N^{ε}-trimethylated lysine surrogates (peptides **2**–**7**) (Table 1), since they share the same primary sequence. Therefore, we have performed an extensive NMR investigation to elucidate whether the structural differences between CA(1–7)M(2–9) and its analogues correlate with the variation of their respective hemolytic activities. To the best of our knowledge, this is the first time in which a detailed and systematic description of the effect of lysine trimethylation on the activity of antimicrobial peptides has been carried out.

The ^{1}H NMR spectra of CA(1–7)M(2–9) and its six [N^{ε}-K(Me_3)]$_i$-derivatives (i = 0, 1, 2 and 5 are CAM, mono-, di- and pan-trimethylated CA(1–7)M(2–9) derivatives respectively, Table 1, peptides **1**–**7**) in both water and aqueous fluoroalcohol solution (H_2O/TFE 30% *v/v*) were assigned in a sequential manner by using homonuclear 2D NMR spectroscopy.[15]

While spectra of peptides in water solution showed signs of random coil or non-ordered structure (e.g., limited dispersion of amide signals, data not shown), addition of 30% TFE (*v/v*) caused significant changes in the chemical shifts of the ^{1}H NMR signals, suggesting that a conformational switch was induced. The ^{1}H NMR assignments of peptides **1**–**7** are listed in Tables S1–S7 in the Supporting Information.

The key methyl groups of the different N^{ε}-trimethylated lysines could be identified by simple examination of 1D ^{1}H NMR spectra since the methyl signals of N^{ε}-trimethylated lysines do not overlap. Indeed, their chemical shifts strongly depend on their positions in the sequence. The aliphatic regions of the 1D ^{1}H NMR spectra of peptides **1** and **5** are compared in Figure 1, which also shows the assignment of the methyl groups of the N^{ε}-trimethylated lysines of **5**.

As a first step in structural analysis of the peptides, the variations of ^{1}H chemical shift values were monitored, since significant changes might have structural relevance. Thus, the observed αH chemical shifts of peptides **1**–**7** were, on average, upfield of the typical values observed for random coils, as might be expected for helical structures. Furthermore, the chemical shift analysis performed with the CSI program[16] predicted mostly helical conformations (data not shown).

Figure 2 shows representative portions of the NOESY spectrum of mono-trimethylated peptide **3**. The NH,αH region of the NOE spectrum revealed the presence of several medium range NOE cross-peaks with key structural information. Thus, the identification of $d_{\alpha N}$ (*i*,*i*+3) and $d_{\alpha N}$ (*i*,*i*+4) NOE cross-peaks

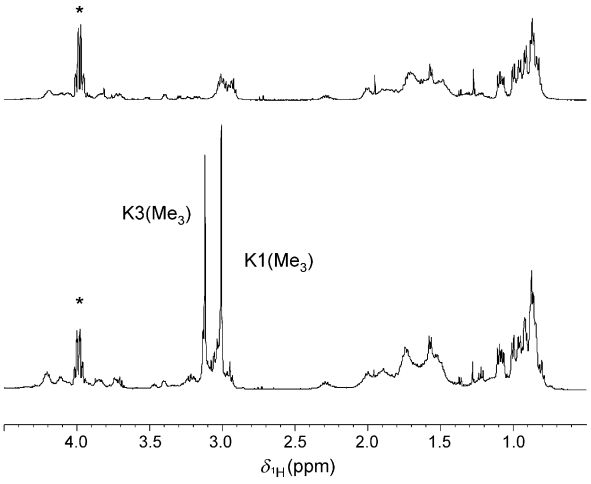

Figure 1. Expansions of 1D ^{1}H NMR spectra (500 MHz) of peptides CA(1–7)M(2–9) (**1**, top) and K1,3(Me_3)$_2$ (**5**, bottom). The asterisk denotes the residual non-deuterated TFE.

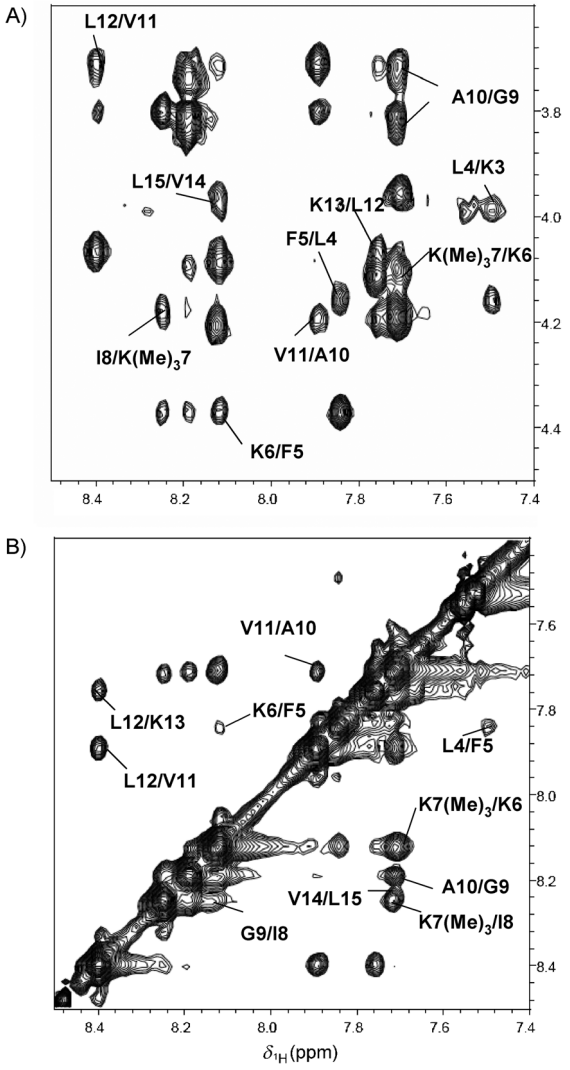

Figure 2. Expansions of 150 ms mixing time NOESY spectrum (500 MHz, 150 ms mixing time) of K7(Me_3) (**3**) in water/TFE (30%, *v/v*) at 298 K. A) Hα–NH sequential NOE cross-peaks. B) NH–NH section showing interactions between amide backbone protons.

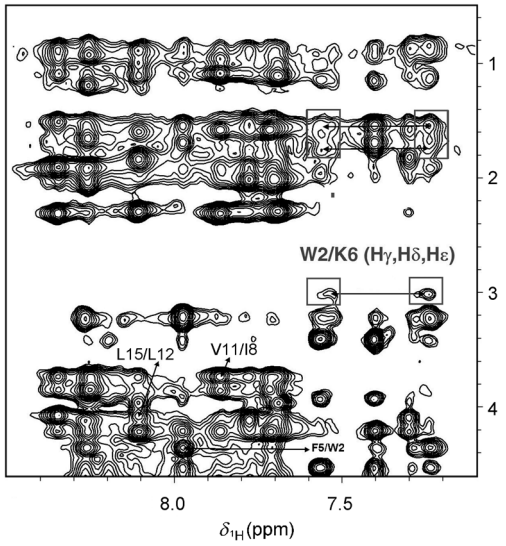

Figure 3. CH–π interactions. Hα–NH region of NOESY spectrum (500 MHz, 150 ms mixing time) of K1,3(Me_3)$_2$ (**5**) in water/TFE (30%, *v/v*) at 298 K showing cross-peaks between aromatic protons of Trp2 and $C^{\beta}H$, $C^{\delta}H$ and $C^{\varepsilon}H$ of Lys6.

[i.e., $d_{\alpha N}$ (W2, F5), $d_{\alpha N}$ (I8, V11), $d_{\alpha N}$ (L12, L15), $d_{\alpha N}$ (V11, L15)], together with the detection of a strong and almost uninterrupted NH,NH (*i*,*i*+1) cross-peak pattern (Figure 2B) are strongly indicative of the presence of a secondary helical structure. In addition, the measured $^3J_{NH\alpha}$ values ranging between 3.5 and 6.0 Hz (Tables S1–S7), support this conclusion.

Furthermore, a significant number of NOE cross-peaks between aromatic protons of residues W2 and F5 and aliphatic protons were found, which represent an additional contribution to structure stabilization of the peptides. On one hand, some weak but measurable spatial connectivities between residues W2 and K6 were identified (Figure 3, peptide **5**). This evidence reflects an interesting contribution by cation–π interactions to the conformational stabilization of this geometry.[17] Indeed, some characteristic signals of the indole of W2 in the aromatic region exhibited extensive contacts with the side chain of K6 (Hγ, Hδ and Hε) as evidenced in the NOE cross-peaks highlighted in Figure 3. One energy-minimized structure of **2** is displayed in Figure S1, which also shows the cation–π interactions between W2 and K6. In addition, many other NOE cross-peaks were assigned to aromatic–aliphatic proton pairs, which might be considered as sensors of the presence of stabilizing CH–π interactions.[18]

Temperature coefficients of the amide protons were then inspected. Although caution should be taken when considering this NMR parameter, since the dependence of amide chemical shifts on the temperature also changes with solvent composition,[19] it has been established that temperature coefficients ($\Delta\delta_{HN}/\Delta T$) might correlate with the presence of intramolecular hydrogen bonds (e.g., between CO and NH of amino acids)[20] and, consequently, with the occurrence (or not) of a well-defined secondary structure. Typically, small temperature coefficients (e.g., < 6 ppb K^{-1}) indicate that the corresponding amide hydrogen participates as a donor in a hydrogen bond. Temperature coefficients of peptides **1**–**7** are listed in the assignment tables (Tables S1–S7). In general, temperature coefficients values were fairly small, suggesting the existence of intramolecular hydrogen bonds and, therefore, of secondary structure.

Finally, the comparison of the chemical shift values of the ε-CH_2 protons of the N^{ε}-trimethylated lysine residues for peptides **2**–**7** were noticeably downfield of those of the parent peptide **1** (Figure S2). These data suggest that, for N^{ε}-trimethylated lysines, the positive (cationic) charge of the amine is not only buried into a hydrophobic core (methyl and ε-CH_2 groups) but is also more dispersed than in the case of lysine residues. In principle, this arrangement might weaken the interaction of the cationic peptide with the anionic prokaryotic membranes.

It has been proposed that AMP aggregation might follow the initial interaction of AMPs with their target membranes and, therefore, play an important role in the AMPs mode of

action.[21] However, in the present study, the existence of aggregation is unlikely as 1) long-range distance NOEs (>5 residues) representative of intermolecular interactions are absent, and 2) no line-broadening of signals (characteristic of oligomerization) was observed upon addition of TFE. Therefore, our data do not support the presence of peptide aggregation in water/TFE, despite a previous report on self-association for CA(1–7)M(2–9) in HFIP.[22] This discrepancy might be attributed to the different experimental conditions (i.e., pH, solvent and cosolvent) employed in these studies.

Three-dimensional structure of peptides 1–7

The experimental NMR data were used to generate three-dimensional models of the peptides. Thus, structural calculations based on inter-proton distance restraints (NOE intensities) were carried out. The statistics regarding the quality and precision of the 20 energy-minimized conformers that represent the solution structure of each of the peptides **1**–**7** are summarized in Table S8. The structures of **1**–**7**, superimposed along their backbone, are shown in Figures 4 and 5. As can be seen, peptides mostly adopt an α-helical conformation. However, this tendency depends on the sequence and, in general, it is maximal for the C terminus (melittin segment) and frayed at the N terminus (cecropin fragment).

The Edmundson projection of CA(1–7)M(2–9) (**1**) displayed in Figure 4 reveals the amphipathic nature of such α-helical structure, with polar (Lys) and nonpolar (Leu, Val, Phe) residues oriented along the opposing faces of the long axis of the helix.

Figure 5 gathers the 3D structures of peptides **2**–**7** in solution. In general, the occurrence of N^{ε}-trimethylated lysines confers a certain degree of local flexibility of the α-helix. Thus, when the N^{ε}-trimethylated lysines are located near the N and/or C terminus [i.e., for peptides **2**, **4**, and **5** (cecropin fragment), or for peptide **6** (both cecropin and melittin fragments)], there is almost no conformational impact, when compared to the structures of peptides with modified lysines at the middle of the sequence (i.e., peptides **3** and **7**).

Indeed, peptide **7** exhibits a helical structure with a large degree of flexibility in both fragments. In principle, this striking

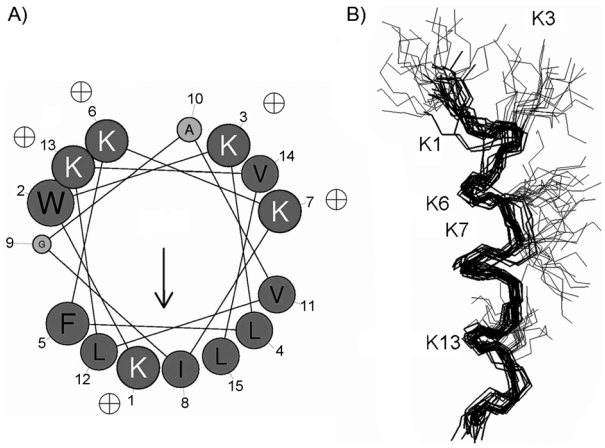

Figure 4. A) Edmundson projection of **1** [CA(1–7)M(2–9)]. Charged residues are indicated. B) Overlapping of the 20 energy-minimized structures of **1** as calculated from NMR data obtained at 298 K in water/TFE solution (30%, *v/v*). The structures are superimposed over the backbone atoms N,Cα and C of residues 1–15.

variation could preclude the effective interaction of the peptide with both bacterial and eukaryotic membranes. Therefore, it is our educated guess that a relative disorder of the helical structure together with the intrinsic steric hindrance of the three methyl groups (bulk/hydrophobicity) and a relative dispersion of the cationic charge mentioned above, would impede membrane–peptide interaction.

In contrast, peptides **2**–**6**, whose structures remain highly helical and stable, exhibited significant antibiotic and hemolytic activities. It is tempting to conclude that at least a threshold helicity seems to be essential for maintaining the proper orientation and interaction features, and that the melittin fragment would be mostly responsible for the residual hemolytic activity.

The interaction with SDS micelles

The study of the mode of interaction of AMPs with prokaryotic membrane-mimetic models (e.g., SDS micelles, dodecylphosphocholine (DPC) micelles) might help to understand their biological lethal mechanism. A previous study on CA(1–7)M(2–9)

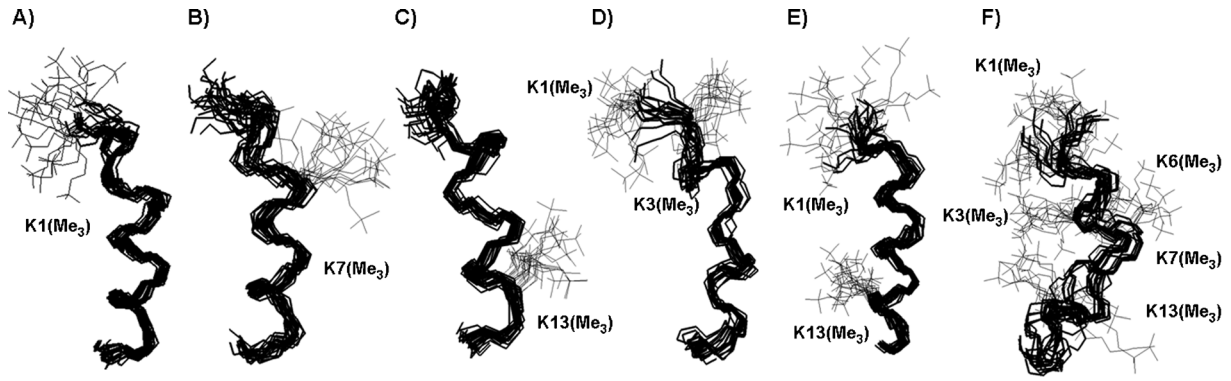

Figure 5. Overlapping of the 20 energy-minimized structures of peptides **2**–**7** as calculated from NMR data obtained at 298 K in water/TFE solution (30%, *v/v*). The structures are superimposed over the backbone atoms N, Cα and C of residues 1–15. A) **2** [K1(Me_3)], B) **3** [K7(Me_3)], C) **4** [K13(Me_3)], D) **5** [K1,3(Me_3)$_2$], E) **6** [K1,13 (Me_3)$_2$] and F) **7** [K1,3,,6,7,13(Me_3)$_5$]. The N^{ε}-trimethyllysine side chain is shown in gray.

and a set of spin-labeled surrogates by using electron paramagnetic resonance (EPR), proposed the induction of a single α-helix after contact with phospholipid membranes, with subsequent insertion of the peptide into membrane as a final outcome.[23] More recently, the combined use of differential scanning calorimetry (DSC) and fluorescence spectroscopy methods have allowed the demonstration that several trimethylated lysine analogues of peptide CA(1–7)M(2–9) strongly interact with negatively charged phospholipidic membranes, but not with eukaryotic model liposomes (zwitterionic lipids). In this context, a proposal for the mechanism of membrane permeabilization of the parental peptide has been described.[24]

Thus, to provide a complete perspective of the presentation mode of the peptides in a membrane-like environment, additional NMR experiments were performed. In particular, the interaction of peptide **4** with SDS micelles was analyzed in the presence of Mn^{2+} as a paramagnetic probe to monitor the orientation of the different segments of the peptide with respect to the membrane-mimicking medium.[25] Peptide **4** was chosen as a model of the helical family of the CA(1–7)M(2–9)/N^{ε}-KMe_3-CA(1–7)M(2–9) derivatives, as shown above. The NMR samples for spin-label experiments consisted of approximately 2 mM peptide in 60–80 mM [D_{25}]SDS. In the presence of SDS micelles, proton spectra showed significant signal broadening, suggesting an effective interaction between the peptide and the micelle medium. Assignment of the NMR signals as well as structural calculations based on distance restraints were performed and agreed with a predominantly helical conformation of peptide **4** when SDS micelles are present, as occurred in water/TFE mixtures (Tables S9 and S10 and Figure S4). Then, an aqueous solution of $MnCl_2$ was added stepwise to the peptide/SDS sample to reach a final concentration of 0.1 mM. Not all the signals of the peptide were affected in the same manner. Indeed, the increase of the Mn^{2+} concentration was correlated with a progressive, but selective, broadening of some of the NH–Hα resonance cross-peaks in the recorded 2D spectra (Figure 6B). In principle, it is expected that the signals that disappear in the presence of the Mn^{2+} ions belong to those protons which are exposed to the solvent. On the other hand, the intensities of the signals of the residues immersed into the micelle, are protected from the paramagnetic Mn^{2+} probe, and should be less affected.[25]

TOCSY experiments were used to monitor the changes, since they are an easy-to-follow and sensitive structural probe of the different amino acids. It was found that in the TOCSY spectrum the NH–Hα cross-peaks from residues G9A10 and L12K13(Me_3)-V14L15 of the melittin fragment of **4** vanished in the presence Mn^{2+}. In contrast, the intensity of the signals of the residues from the cecropin fragment remained in the spectrum. This fact strongly suggests that this section of the peptide is well-protected from exposure to Mn^{2+}, and therefore in contact with the membrane. It can be concluded that **4** and SDS micelles interact primarily by electrostatic interactions between the cecropin fragment (where most of the cationic charges are located) and the negatively charged head groups of the SDS micelles.

Conclusions

For the whole set of peptides analyzed, the NMR data, assisted by molecular modeling have shown that both cecropin A and melittin fragments adopt a major helical geometry in water/TFE solution. Fittingly, regardless of the chemical nature of the peptide analyzed in this set, the cecropin helical fragment is more disordered than the melittin section. In general, trimethylation in the melittin fragment has a lower structural impact than at the more disordered N terminus.

Although a straightforward correlation between structural data and biological activities is frequently hampered by the complexity of the living organisms, including phospholipid composition and asymmetry of the plasma membrane, with the concomitant presence of other molecular entities, the results of the current work suggest that a critical helicity value of the melittin section of the hybrid peptide, together with electrostatic interactions with the anionic membrane of the targeted microorganism is mandatory to preserve the antimicrobial activity of these peptides. In contrast, hemolytic activity is favored by stabilization of a helical melittin portion, as in peptides **3** [K7(Me_3)] and **4** [K13(Me_3)], respectively. Other factors such as the bulkiness/hydrophobicity of the substituents at the N^{ε} of the lysines and dispersion of the positive charge can also play an important role in finely tuning the activity of the peptides, by selecting key lysines to be substituted by N^{ε}-trimethylated residues. Thus, although generally speaking, structures of AMPs described in literature appear to converge in a similar

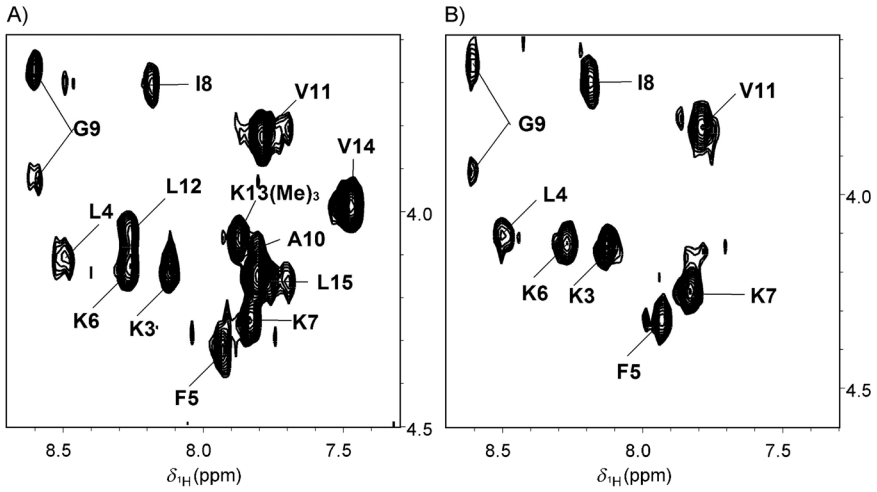

Figure 6. Effect of paramagnetic ions (Mn^{2+}) on NH–Hα signals of peptide **4**. 500 MHz TOCSY spectra of **4** (2 mM) in 80 mM [D_{25}]SDS A) without and B) with 0.1 mM $MnCl_2$ at 298 K.

structure in both water/TFE and in the presence of micelles (e.g., SDS, DPC),[26] current work in our laboratory is attempting to better characterize the 3D structure of peptides as well as the peptide–membrane interaction in the presence of those systems as they can better mimic an in vivo environment.

The positioning of peptide **4** [K13(Me_3)], taken as representative model of the family, with respect to SDS micelles has been probed by the addition of paramagnetic Mn^{2+} ions. The experimental data demonstrate that residues 2–9 (the first six of which belong to the cecropin A fragment) participate directly in the interaction with the micelle. Because this fragment contains the maximum number of charged residues, it can be concluded that the interaction between this peptide and SDS micelles is mainly driven by electrostatic interactions.

Experimental Section

Peptide synthesis and characterization: In brief, peptides were synthesized by Fmoc chemistry protocols as described previously. The detailed methodology as well as characterization of peptides CA(1–7)M(2–9) and its trimethylated derivatives was described previously.[13]

NMR samples: Samples of peptides **1**–**6** (Table 1) for NMR experiments were dissolved in PBS buffer (pH 6.3) or in TFE-containing aqueous solution (30% *v/v* trifluoroethanol-d3, Cambridge Isotope Laboratories) to give a final peptide concentration of approximately 3 mM. Spectra were recorded at 298 K on a Bruker DRX-500 spectrometer (^{1}H frequency of 500 MHz) by using a 5 mm triple-resonance *Z* gradient probe and processed by using XWIN-NMR software (Bruker). The transmitter frequency was set on the HDO/H_2O signal, and trimethylsilyl propionate (TSP) was used as the chemical shift reference ($\delta_{TSP} = 0$ ppm).

The concentrations for perdeuterated SDS samples resulted in a peptide/SDS molar ratio of 1:40. For Mn^{2+} experiments, a stock solution of aq. $MnCl_2$ was added stepwise to the peptide/micelle sample until final $MnCl_2$ concentration was 100 mM. [D_{25}]SDS was purchased from Cambridge Isotopes Laboratories.

NMR experiments: One- and two-dimensional spectra were acquired by using standard pulse sequences and WATERGATE-based solvent suppression sequences. Total correlation spectroscopy (TOCSY) and nuclear Overhauser effect spectroscopy (NOESY) were performed in the phase-sensitive mode by using 512 time-proportional phase increments in t1 for each experiment. The free induction decay in t2 consisted of 2 K complex data points over a spectral width of 6009.615 Hz. Typically, 4096×1024 data points were collected for each block and 96 transients were collected for two-dimensional experiments. The spectral width was 14 ppm, and the relaxation delays were set to 1.5 and 2 s in the TOCSY and NOESY experiments, respectively. TOCSY spectra were recorded by using the MLEV-17 pulse sequence with mixing times (spin-lock) of 65–80 ms. NOESY experiments were acquired with mixing time of 150–200 ms to avoid any possible contribution from spin diffusion. The NH-CαH scalar couplings were obtained from high-resolution 1H-monodimensional spectra. The experimental data were acquired and processed by using the XWIN-NMR/Topspin software (Bruker) on a PC station. The data matrices were multiplied by a qsine function in both dimensions and then zero-filled to 1024 data points in F1 prior to Fourier transformation.

$^3J_{NH-H\alpha}$ coupling constants for non-overlapping signals were obtained from the amide region of the 1D spectra with high digital resolution recorded at 298 K.

The temperature coefficients of the backbone amide resonances of CA(1–7)M(2–9) and its derivatives were measured from 2D TOCSY spectra recorded at 298 and 288 K. Temperature coefficients ($\Delta\delta/\Delta T$) for backbone amide protons (NH) were calculated from linear plots of NH chemical shift versus temperature.

Structure calculation: Peak lists for the NOESY spectra recorded with a 0.15–0.2 s mixing time were generated by interactive peak picking using the CARA software.[27] NOESY cross-peak volumes were determined by the automated peak integration routine implemented in CARA. 3D structures were determined by the standard protocol of the CYANA program (version 2.1),[28] using seven cycles of combined automated NOESY assignment and structure calculations followed by a final structure calculation. Since the N^{ε}-trimethylated lysine residue is not included in the standard CYANA libraries, it was built by using the MOLMOL program[29] which was also used to visualize the 3D structures.

For each CYANA cycle, 1000 randomized conformers and the standard simulated annealing schedule were used. The 20 conformers with the lowest final score were retained for analysis and passed on to the next cycle. Weak restraints on ϕ/ψ torsion-angle pairs and on side-chain torsion angles between tetrahedral carbon atoms were applied temporarily during the high-temperature and cooling phases of the simulated annealing schedule in order to favor the permitted regions of the Ramachandran plot and staggered rotamer positions, respectively. The list of upper- distance bonds for the final structural calculation consists of unambiguously assigned upper-distance bonds and does not require the possible swapping of diastereotopic pairs.

Next, the 20 conformers with the lowest final CYANA target function values were subjected to restrained energy-minimization in a water shell by using the AMBER 8.0 program.[30] The protein was immersed in a shell of water molecules created by using the TIP3P model, with a thickness of 10 Å. The restrained energy minimization was performed in three stages. In the first stage, only the water molecules were optimized. Subsequently, the peptide alone was relaxed, maintaining the water molecules fixed, and, finally, the whole system was minimized. In the last stage, a maximum of 1500 steps of restrained energy minimization and a combination of the steepest descent and conjugate gradient algorithms were applied by using, in addition to the force field of Cornell et al.,[31] a parabolic or linear penalty function for the NOE upper distance bonds and torsion-angle restraints. The resulting 20 energy-minimized conformers represent the solution structure of peptides **1**–**7** and were selected for further analysis.

Root-mean-square deviation (rmsd) values were calculated by using CYANA for superpositions of the backbone N, Cα, and CO atoms; the heavy atoms over the whole peptide. To obtain the rmsd of a structure represented by a bundle of conformers, all conformers were superimposed upon the first one and the average of the rmsd values between the individual conformers and their average coordinates was calculated. The statistics regarding the quality and precision of the 20 energy-minimized conformers that represent the solution structure of peptides **1**–**7** are summarized in Table S8.

Hydrogen bonds were identified in MOLMOL by using a maximum distance of 2.4 Å and a maximum angular deviation of 35° from linearity. The quality of these structures was validated by using the

ADIT validation server at RCSB-Rutgers[32] and was supported by the presence of 73.8–92.7% of the ϕ/ψ backbone torsion-angle pairs in the most favored regions and 7.3–26.2% of which within the regions additionally permitted by the Ramachandran plot, according to PROCHECK conventions.[33]

Acknowledgements

M.D.D. gratefully acknowledges support through a "Ramón y Cajal" contract from Ministerio de Ciencia e Innovación (MICINN) of Spain. J.J.B. thanks also MICINN for financial support (grant CTQ2009-08536). L.R. is supported by projects FIS 09/01928, RD 06/0021/0006 and EC HEALTH M-2007-223414. We also thank CESGA (Santiago de Compostela) for computer support.

Keywords: antimicrobial peptides (AMPs) · cecropin A · membranes · NMR spectroscopy · trimethyllysine

[1] a) D. Andreu, L. Rivas, *Biopolymers* **1998**, *47*, 415–433; b) M. Zasloff, *Nature* **2002**, *415*, 389–395.
[2] D. Andreu, J. Ubach, A. Boman, B. Wahlin, D. Wade, R. B. Merrifield, H. G. Boman, *FEBS Lett.* **1992**, *296*, 190–194.
[3] L. H. Kondejewski, M. Jelokhani-Niaraki, S. W. Farmer, B. Lix, C. M. Kay, B. D. Sykes, R. E. W. Hancock, R. S. Hodges, *J. Biol. Chem.* **1999**, *274*, 13181–13192.
[4] a) M. Dathe, T. Wieprecht, H. Nikolenko, L. Handel, W. L. Maloy, D. L. MacDonald, M. Beyermann, M. Bienert, *FEBS Lett.* **1997**, *403*, 208–212; b) S. E. Blondelle, R. A. Houghten, *Biochemistry* **1992**, *31*, 12688–12694; c) Z. Oren, J. Hong, Y. Shai, *J. Biol. Chem.* **1997**, *272*, 14643–14649; d) Y. Shai, Z. Oren, *J. Biol. Chem.* **1996**, *271*, 7305–7308; e) Z. Oren, Y. Shai, *Biochem.* **1997**, *36*, 1826–1835; f) M. Dathe, M. Shumann, T. Wieprecht, A. Winkler, M. Beyermann, E. Krause, K. Matsuzaki, O. Murase, M. Bienert, *Biochemistry* **1996**, *35*, 12612–12622.
[5] D. Sipos, K. Chandrasekhar, K. Arvidsson, A. Engstrom, A. Ehrenberg, *Eur. J. Biochem.* **1991**, *199*, 285–291.
[6] a) H. Oh, M. Hedberg, D. Wade, Ch. Edlund, *Antimicrob. Agents Chemother.* **2000**, *44*, 68–73; b) D. Oh, S. Y. Shin, J. H. Kang, K.-S. Hahm, K. L. Kim, Y. Kim, *J. Peptide Res.* **1999**, *53*, 578–589.
[7] I. Fernández, J. Ubach, M. Fuxreiter, J. M. Andreu, D. Andreu, M. Pons, *Chem. Eur. J.* **1996**, *2*, 838–846.
[8] I. Fernández, J. Ubach, F. Reig, D. Andreu, M. Pons, *Biopolymers* **1994**, *34*, 1251–1258.
[9] C. Chicharro, C. Granata, R. Lozano, D. Andreu, L. Rivas, *Antimicrob. Agents Chemother.* **2001**, *45*, 2441–2449.
[10] a) P. Mathur, N. R. Jagannathan, V. S. Chauhan, *J. Pept. Sci.* **2007**, *13*, 253–262; b) H. Oh, M. Hedberg, D. Wade, Ch. Edlund, *Antimicrob. Agents Chemother.* **2000**, *44*, 68–73.
[11] a) B. C. Smith, J. M. Denu, *Biochim. Biophys. Acta Gene Regul. Mech.* **2009**, *1789*, 45–57; b) B. E. Haug, M. B. Strom, J. S. Svendsen, *Curr. Med. Chem.* **2007**, *14*, 1–18.
[12] a) K. Ramalingam, J. Bello, *Biochem. J.* **1992**, *284*, 663–665; b) K. Ramalingam, J. Bello, S. Aimoto, *Biopolymers* **1993**, *33*, 305–314.
[13] M. Fernández-Reyes, M. D. Díaz, B. G. de La Torre, A. Cabrales-Rico, M. Vallés-Miret, J. Jiménez-Barbero, D. Andreu, L. Rivas, *J. Med. Chem.* **2010**, *53*, 5587–5596.
[14] R. M. Kini, H. J. Evans, *Int. J. Peptide Protein Res.* **1989**, *34*, 277–286.
[15] K. Wüthrich, *NMR of Proteins and Nucleic Acids*, Wiley, New York, **1986**.
[16] a) D. S. Wishart, F. M. Richards, B. D. Sykes, *J. Mol. Biol.* **1991**, *222*, 311–333; b) D. S. Wishart, F. M. Richards, B. D. Sykes, *Biochemistry* **1992**, *31*, 1647–1651; c) Residue N^{ε}-trimethyllysine is not reported in CSI, therefore, for CSI calculations N^{ε}-trimethyllysine has been substituted by lysine (http://www.bionmr.ualberta.ca/bds/software/csi/latest/csi.html).
[17] Z. Shi, C. A. Olson, N. R. Kallenbach, *J. Am. Chem. Soc.* **2002**, *124*, 3284–3291.
[18] M. C. Fernandez-Alonso, F. J. Cañada, J. Jiménez-Barbero, G. Cuevas, *J. Am. Chem. Soc.* **2005**, *127*, 7379–7386.
[19] a) S. Rothemund, H. Weisshof, M. Beyermann, E. Krause, M. Bienert, C. Muegge, B. D. Sykes, F. D. Soennischen, *J. Biomol. NMR* **1996**, *8*, 93–97; b) N. H. Andersen, J. W. Neidigh, S. M. Harris, G. M. Lee, Z. Liu, H. J. Tong, *J. Am. Chem. Soc.* **1997**, *119*, 8547–8561.
[20] a) H. J. Dyson, M. Rance, R. A. Houghten, R. A. Lerner, P. E. Wright, *J. Mol. Biol.* **1988**, *201*, 161–200; b) T. Cierpicki, J. Otlewski, *J. Biomol. NMR* **2001**, *21*, 249–261.
[21] M. R. Yeaman, N. Y. Yount, *Pharmacol. Rev.* **2003**, *55*, 27–55.
[22] I. Fernández, J. Ubach, D. Andreu, M. Pons, *Colloids Surf.* **1996**, *115*, 39–45.
[23] K. Bhargava, J. B. Feix, *Biophys. J.* **2004**, *86*, 329–336.
[24] V. Teixeira, M. J. Feio, L. Rivas, B. G. De La Torre, D. Andreu, D. Bastos, *J. Phys. Chem. B* **2010**, *114*, 16198–16208.
[25] a) J. Jarvet, J. Danielsson , P. Damberg, M. Oleszczuk, A. Gräslund, *J. Biomol. NMR* **2007**, *39*, 63–72; b) P. Damberg, J. Jarvet, A. Gräslund, *Methods Enzymol.* **2001**, *339*, 271–285.
[26] a) E. F. Haney, H. N. Hunter, K. Matzusaki, H. J. Evans, *Biochim. Biophys. Acta Biomembr.* **2009**, *1788*, 1639–1655; b) E. Strandberg, A. S. Ulrich, *Concepts Magn. Res. Part A* **2004**, *23*, 89–120; c) J. Boisbouvier, A. Prochnicka-Chalufour, A. R. Nieto, J. A. Torres, N. Nanard, M. H. Rodriguez, L. D. Possani, M. Delepierre, *Eur. J. Biochem.* **1998**, *257*, 263–273; d) H. Sato, J. B. Feix, *Biochim. Biophys. Acta Biomembr.* **2006**, *1758*, 1245–1256; e) S. Pistolesi, R. Pogni, J. B. Feix, *Biophys. J.* **2007**, *93*, 1651–1660; f) C. Landon, H. Meudal, N. Boulanger, P. Bulet, F. Vovelle, *Biopolymers* **2006**, *81*, 92–103.
[27] R. L. J. Keller, *The Computer Aided Resonance Assignment Tutorial*, Cantina, Goldau, **2004**.
[28] P. Güntert, *Methods Mol. Biol.* **2004**, *278*, 353–378.
[29] R. Koradi, M. Billeter, K. Wüthrich, *J. Mol. Graphics* **1996**, *14*, 51–55.
[30] a) D. A. Case, T. A. Darden, T. E. Cheatham III, C. L. Simmerling, J. Wang, R. E. Duke, R. Luo, K. M. Merz, B. Wang, D. A. Pearlman, M. Crowley, S. Brozell, V. Tsui, H. Gohlke, J. Mongan, V. Hornak, G. Cui, P. Beroza, C. Schafmeister, J. W. Caldwell, W. S. Ross, P. A. Kollman, **2004**, AMBER 8, University of California, San Francisco; b) F. Y. Dupradeau, A. Pigache, T. Zaffran, C. Savineau, R. Lelong, N. Grivel, D. Lelong, W. Rosanski, P. Cieplak, *Phys. Chem. Chem. Phys.* **2010**, *12*, 7821–7839.
[31] W. D. Cornell, P. Cieplak, C. I. Bayly, I. R. Gould, K. M. Merz, D. M. Ferguson, *J. Am. Chem. Soc.* **1995**, *117*, 5179–5197.
[32] http://psvs-1_4-dev.nesg.org/
[33] R. A. Laskowski, M. W. MacArthur, D. S. Moss, J. M. Thornton, *J. Appl. Crystallogr.* **1993**, *26*, 283–291.

Received: April 27, 2011
Published online on July 29, 2011

